The FIRST-SPIRE Spectrometer
A Novel Imaging FTS for the Sub-Millimetre

Bruce. M. Swinyard[*a], Peter Ade[b], Matthew J. Griffin[b], Kjetil Dohlen[c], Jean-Paul Baluteau[c], Dominique Pouliquen[c], Didier Ferand[c], Pascal Dargent[c], Guy Michel[d], Jerome Martignac[e], Louis Rodriguez[e], Donald Jennings[f], Martin Caldwell[a], Anthony Richards[a], Peter Hamilton[b], David Naylor[g]

[a]Rutherford Appleton Laboratory, Chilton, Didcot, Oxon, OX11 0QX, U.K.
[b]Queen Mary and Westfield College, University of London, Mile End Road, London, E1 4NS, U.K.
[c]Laboratoire d'Astrophysique de Marseille, BP 8 13376, Marseille, France,
[d]Observatoire de Meudon, 5 Place Jules Janssen, 92195, Meudon Cedex, Paris, France,
[e]CEA-Service d'Astrophysique, Bât. 709, Orme des Merisiers, 91191 Gif sur Yvette, France.
[f]Goddard Space Flight Center, Greenbelt, MD, 20771, U.S.A,
[g]University of Lethbridge, Lethbridge, Alberta T1K 3M4, Canada.

ABSTRACT

The SPIRE instrument for the FIRST mission will consist of a three band imaging submillimetre photometer and a two band imaging Fourier Transform Spectrometer (FTS) optimised for the 200-400 μm range, and with extended coverage out to 670 μm. The FTS will be used for follow-up spectroscopic studies of objects detected in photometric surveys by SPIRE and other facilities, and to perform medium resolving power (R~500 at 250 μm) imaging spectroscopy on galactic and nearby extra-galactic sources.

The FTS is of a novel design for the far infrared and sub-millimetre regime as is uses twin broadband intensity beam splitters in a Mach-Zehnder configuration rather than the traditional polarising beam splitters. This arrangement means that all four ports are still accessible whilst maintaining the maximum throughput and removing any polarisation sensitivity. The performance of this design has been demonstrated using a laboratory system. The overall design of the FTS is described together with the design of the novel beam splitters. The performance of the laboratory instrument is reported together with results of the simulated performance of the flight design.

Keywords: Instrumentation, far infrared, spectrographs, Fourier Transform Spectrometer, space

1. INTRODUCTION

The Far Infrared and Submillimetre Telescope (FIRST) mission[1] is dedicated to observing the cosmos at wavelengths from 85 to 700 μm. It consists of a 3.5 m telescope at a temperature of 80 K with a suite of focal plane instruments cooled to <11 K in a liquid helium cryostat. The SPIRE instrument[2] is one of the three focal plane instruments for FIRST. It will make observations in the 200 to 670 μm band using bolometer detectors. The focal plane unit of SPIRE is operated at cryogenic temperature (<11 K) and the NTD Germanium bolometer feedhorn arrays[3] are operated at ~300 mK. This temperature is provided by a ^{3}He sorption cooler. The instrument has two sub-instruments: a multi-frequency imaging photometer using three separate bolometer arrays with resolving power of about $\lambda/\Delta\lambda \sim 3$, and an imaging Fourier Transform Spectrometer (FTS) that provides a maximum resolving power of 1000 at 250 μm.

The photometer will simultaneously image a 4x8 arcmin field of view onto spectral bands nominally centred on 250, 350 and 500 μm. A beam steering mirror will be used to move or spatially modulate the source image at the detector arrays. To give complete spatial sampling of the field of view the image needs to be sequentially stepped by fractions of the Airy pattern diameter. The spectrometer uses two bolometer arrays to give spectrally resolved images of a small (~2.6 arcmin) area of sky. The two bolometer arrays have nominal optical bands of 200-300 and 300-670 μm. The spectrometer shares the input optics of the instrument with the photometer, including the beam steering mechanism. This paper discusses the

[*] contact for more information and pre-prints: B.M.Swinyard@rl.ac.uk

design; operation and predicted performance of the SPIRE FTS. Further details of the design of the whole instrument can be found in reference 2; details of the optical design in reference 4 and the diffraction limited performance of the instrument in reference 5.

2. CHOICE OF SPECTROMETER TYPE

One of the primary science goals for the SPIRE instrument is large area surveys (many 10's of square degrees) using the photometer to enable the detection and location of high redshift galaxies through observation of the FIR and sub-millimeter radiation emitted from stellar UV radiation reprocessed via the interstellar dust in those galaxies. Although large numbers of objects will be found in these surveys, the determination of an individual object's redshift using just the three photometric bands would be subject to some uncertainty due to a) it being model dependent and b) that not all objects will be detected in all of the bands. A spectrometer is therefore required to follow up the sources detected in the photometric survey to enable either a more precise determination of the spectral shape using narrow band spectro-photometry ($\lambda/\Delta\lambda \sim 20$) or the identification of redshifted FIR atomic fine structure lines, most notably CII(157μm); OI(63μm); OI(145μm) and NII(205μm), that are known to arise in the star formation regions of our own and nearby galaxies. These lines should be present in the spectra of all galaxies undergoing active star formation. A spectral resolving power of a few hundred is sufficient to allow unambiguous detection of this type of line, and, because the redshift, and therefore the wavelengths at which the lines will be seen, is unknown, an ability to rapidly spectrally survey a wide wavelength range is essential.

One of the other major science goals of SPIRE is to advance the understanding of the early evolution of star formation in our own and nearby galaxies. Experience from the Infrared Space Observatory in observing galactic star formation regions has shown that good spatial resolution is essential for both photometric and spectroscopic observations as these regions contain gas and dust at different temperatures and ionisation states with relatively small angular separation. Spatial confusion due to the modest angular resolution of the ISO telescope at FIR wavelengths (~80 arcsec) has thus severely limited the interpretation of the data. Although most of the important cooling lines (CII(157μm),OI(145μm), OIII(88μm) etc) fall in the FIRST PACS instrument wavelength range[6], the NII(205μm) and the CI(370μm) atomic lines will be within the range of the SPIRE spectrometer as well as many molecular lines and, if the final design permits, the important CI(609μm) ground state transition. The FIRST HIFI instrument will also have access to these lines with very high spectral resolution, and thus velocity discrimination, but with limited spatial coverage per observation. An instrument with modest spectral resolving power of order 500, but with a direct imaging capability, covering at least the 200 to 400 μm band was therefore felt to be a natural complement to the HIFI and PACS instruments.

In choosing the type of spectrometer to implement the following factors and requirements were considered:

- The radiation background due to the 80 K 4% emissive telescope
- The need for wide spectral coverage – at least 200 to 400 μm with a goal of 200 to 650 μm
- The need for a resolving power of at least 100 over as much of the wavelength range as possible
- The ability to have variable spectral resolving power or to be able to bin the spectra to any given, broader, resolution without incurring a signal to noise penalty
- The requirement to have diffraction limited spatial resolution over the 200 to 400 μm band.
- The desirability of having a large instantaneous field of view
- The necessity of having both the maximum sensitivity possible and to cover the available spectral range as rapidly as possible.
- The difficulty in predicting and controlling the straylight environment within the SPIRE instrument.

The initial design of the SPIRE instrument[7] envisaged a dilution refrigerator to cool the bolometer array to a temperature of 100 mK similar to that used on the Planck HFI intrument[8]. This offered the possibility of having detector NEP's of $\leq 1 \times 10^{-17}$ W $Hz^{-1/2}$. This in turn meant that the use of a monochromating spectrometer could be contemplated such as a tandem Fabry-Perot or a diffraction grating to spectrally band limit the detectors and thus reduce the radiation from the telescope and increase the sensitivity. A Fabry-Perot spectrometer was rejected early on because to achieve the broad spectral coverage inevitably meant using more than one Fabry-Perot mounted on an interchange wheel. An early conceptual design of the instrument showed that three such wheels would be necessary resulting in an overly complex instrument design. A grating spectrometer was therefore adopted as the baseline, although it could only image in one axis.

As the design of the instrument progressed it was recognised that the adoption of a ^{3}He cooler would very much simplify the instrument and FIRST cryostat design and would also give a longer lifetime as there would be no additional instrument consumables. This choice meant that the achievable detector NEP rose from $1x10^{-17}$ to $3x10^{-17}$ W $Hz^{-1/2}$. Further design evolution of the grating spectrometer concept also showed that, within the space available at the FIRST focal plane the spectrometer would only be capable of achieving a resolving power of around 400 over, at most, a wavelength range of 200 to 400 μm. Also it would, if the straylight could be reduced to the level of 10-20 femtowatts, be detector noise limited. Furthermore, the choice of slit size is difficult as one would either have to sacrifice spatial resolution at the shortest wavelengths, or throughput at the longest wavelengths as a slit plate or variable slit width was considered too complex to implement.

A comparison of the likely achievable sensitivity for the grating design and a nominal polarising Martin-Puplett FTS, showed that, although the grating would be nominally more sensitive, especially for detection of lines at known wavelengths, the difference was only a factor of 2 to 3. It was felt that the loss in instantaneous sensitivity to unresolved lines at known positions was more than offset by the advantages of an FTS namely:

- Diffraction limited spectral imaging over a large field of view
- Large spectral coverage and instantaneous coverage of the whole spectral range
- Variable spectral resolving power
- Immunity to straylight and spectral contamination

3. THE SPIRE FTS

The recent development of broad band intensity beam splitters covering the 200 to 700 μm band[9] – see section 4 - offers the possibility of increasing the sensitivity of the SPIRE spectrometer over the polarising type FTS as the loss of 50% of the input radiation is avoided. These beam splitters offer the possibility of implementing a Mach-Zehnder type design; this has the advantage over the traditional Michelson that all four ports of the spectrometer are available[4]. This, in turn, means that a calibration source can be placed in the second input port with the same spectral characteristics as the telescope. A complementary spectrum of the "telescope" is then seen in the output ports which will null the central maximum at zero path difference (ZPD), thus reducing the requirements on the detector dynamic range and position jitter noise – see discussion in reference 4 and section 7. In the SPIRE design, the two output ports are band limited to 200 to 300 μm and 300 to 670 μm to reduce the background radiation from the telescope. The choice of the passbands was made so as to have approximately the same background loading on each bolometer array.

3.1 OPTICAL DESIGN

The outline optical configuration is shown in figure 1 and the optical design as implemented in the SPIRE instrument in figure 2. We give here an outline description of the optical design, the detailed optical design is discussed in reference 4. After reflection from the input mirrors M3, M4, and M5, which are common with the photometer optics, the spectrometer beam is picked off by M6s and sent out of the plane of the photometer system. The flat M7s redirects it into a parallel plane, separated by 170 mm from the photometer plane. The input relay mirror (Rin) focuses the beam to an intermediate image plane located just after the first beam splitter, after which the beam is collimated (Coll) and sent vertically towards the corner cube assembly. The corner cube shifts the beam and sends it up towards the camera mirror (Cam). Symmetrical with the collimator, the camera focuses the beam to an image plane just before the output beam splitter. The output relay mirror (Rout) focuses the beam onto the detector arrays. To accommodate the components within the available volume, a fold mirror is needed to take the beam out of the plane again. This configuration allows a single mirror mechanism to be employed for both arms of the interferometer and achieves a folding of a factor of four in the optical path difference with respect to the actual movement of the mirrors.

All the powered mirrors and the mirror mechanism will be mounted from a common optical bench panel at 4 K (see figure 3). The final fold mirror and the detector assemblies will be mounted from a thermally isolated box strapped to the FIRST cryostat liquid helium tank at 1.7 K. A pupil image is located near the final fold mirror, making this a convenient place for the entrance aperture into the 1.7-K enclosure. This pupil moves as the OPD changes, however, so it is not appropriate for a limiting cold stop. Instead, a pupil stop is placed at 4 K between M6s and M7s.

In order to control the out of band radiation entering the instrument, filters will be placed at the entrance to the common optics box; at the instrument entrance aperture at 4 K; at the entrance to 1.7 K enclosure and finally band limiting filters will

be placed directly in front of the bolometer arrays at 300 mK. The beam splitters themselves will also have some limited out of band rejection capabilities.

The optical design has been analysed to evaluate both its geometrical and its diffraction limited imaging performance. The geometrical quality gives a maximum *rms* wave front error of 7 μm, a Strehl ratio greater than 0.97 across the FOV and a distortion of no more than 6%. The feedhorns for the 200-300 μm band will be designed to give a single Gaussian mode illumination of the instrument pupil. The design of the feedhorns for the 300-670 μm band will be challenging as they will have to provide good efficiency over a large spectral band. A design has been proposed that gives single mode performance at the long wavelength end of the band with multi-moded operation at the shortwavelength end. An analysis of the performance of the spectrometer with this type of horn[5] has shown that this will only slightly increase the beam on sky at the short wavelengths and will have a coupling efficiency to the telescope at the longwavelength end of the band of about half that of the single mode at 350 μm. This design is being studied with a view to improving the control of the multi-mode performance and improving the long wavelength efficiency.

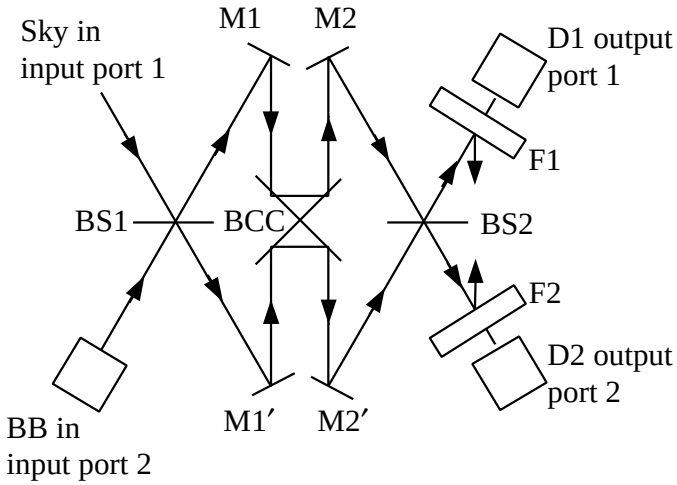

Figure 1. The conceptual design of the SPIRE FTS: the concept is based on a Mach-Zehnder interferometer with its arms folded in order to avoid beam shearing during scanning of the optical path difference (OPD) and uses twin intensity dividing beamsplitters (BS1 and BS2). If the detectors could be used over the entire spectral range, this concept would provide 100% efficiency, but the requirement for two separate bands imposes a 50% channel separation loss. The folding allows the optical path of both arms to be changed simultaneously with a single scanning mechanism, hence doubling the available resolving power for a given moving mirror mechanism. BB: blackbody source, F: filter, D: detector, BS: beamsplitter, M: mirror, BCC: back-to-back corner cubes (or roof-tops).

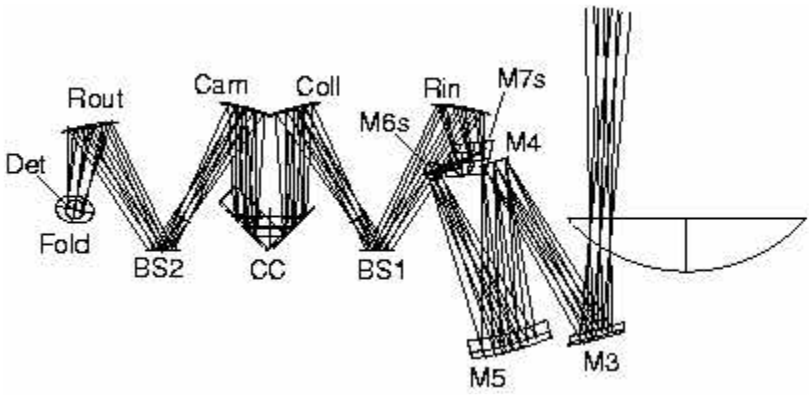

Figure 2. Optical diagram of the upper half of the SPIRE spectrometer. The symmetrical lower half is generated by reflection about the plane containing the two beam splitters.

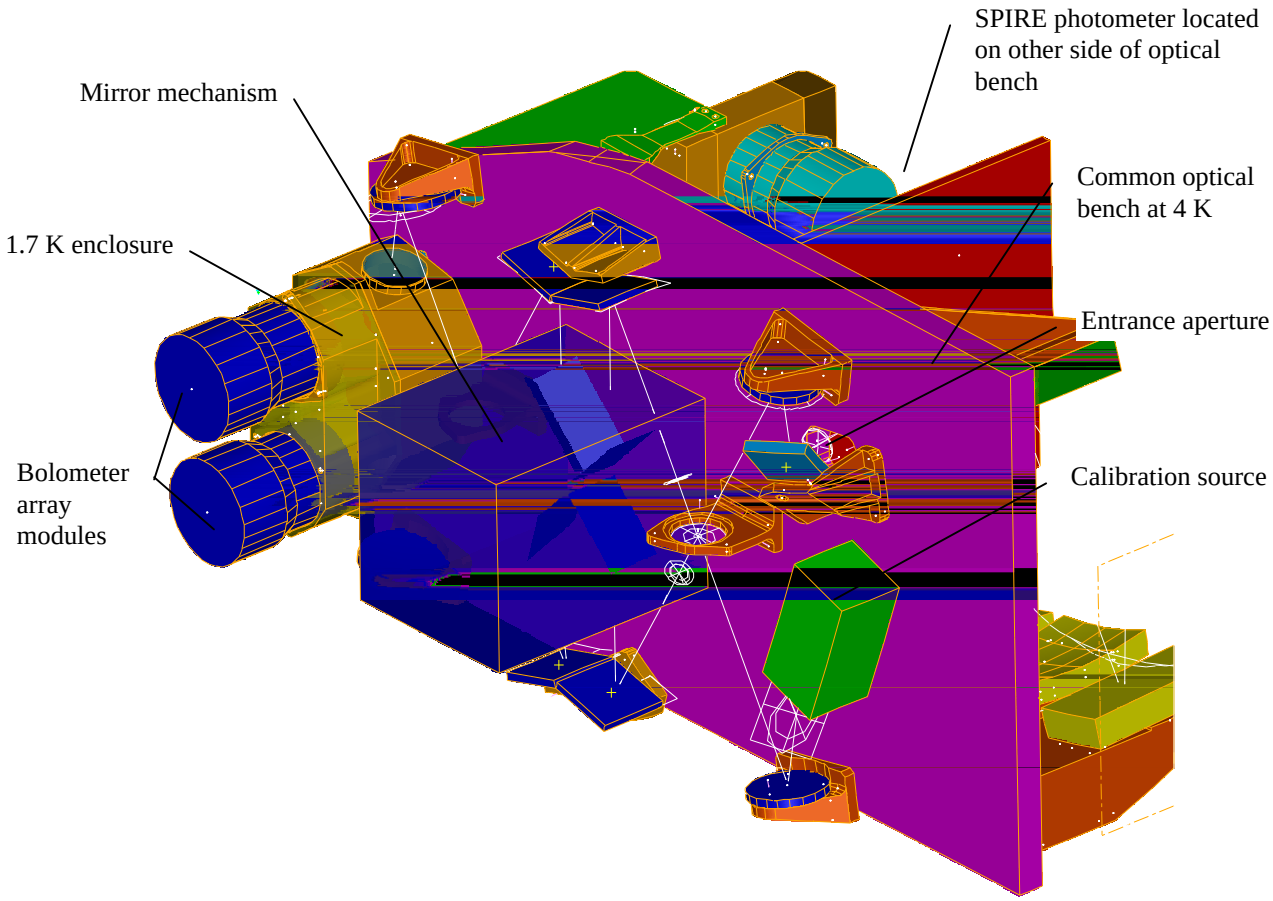

Figure 3: General view of the accommodation of the SPIRE FTS into the common SPIRE structure.

3.2 SPECIFICATION

Optical and instrument design constraints result in the following specification parameters:

Field of view:	2.6 arcmin circular
Strehl ratio at 250 μm	>0.97 over whole field
Throughput excluding beam divider efficiency:	0.4
Wavelength coverage	λ = 200 - 667 μm or 15 - 50 cm^{-1}
	Optimised for operation in 200-400 μm band
Spectral Bands	Band 1 - 200-299 (33 - 50 cm^{-1})
	Band 2 - 299-667 (15 - 33 cm^{-1})
Required resolving power	$\lambda/\Delta\lambda$ = 100 at 250 μm (40 cm^{-1})
Spectral resolution	$\Delta\sigma$ = 0.4 cm^{-1}
Goal for resolving power	$\lambda/\Delta\lambda$ = 1000 at 250 μm (40 cm^{-1})
Maximum spectral resolution	$\Delta\sigma$ = 0.04 cm^{-1}
Required optical path difference for goal resolving power	σ = 1/(2L) $\Rightarrow$ L = 12.5 cm We assume 14 cm for scan length to allow for accurate measurement of zero path difference
Linear travel of mirror mechanism	(14 cm)/4 = 3.5 cm (-0.3 + 3.2 cm)
Nyqvist sampling of optical path difference:	$\Delta x_{max} = 1/(2\sigma_{max})$ $\Rightarrow \Delta x_{max}$ = 1/(2 x 33) = 0.015 cm for band 2 $\Rightarrow \Delta x_{max}$ = 1/(2 x 50) = 0.010 cm for band 1

Audio frequencies	$f = v_{opd}\sigma$ where v_{opd} is the rate of change of the optical path difference.
Maximum allowed audio frequency	20 Hz (from assumed detector response) $\Rightarrow$ $v_{opd} = 20/50 = 0.4$ cm s^{-1}
Maximum mirror velocity	$v_{mirrors} = v_{opd}/4 = 0.1$ cm s^{-1}
Audio freq. band for maximum mirror velocity	15 - 33 cm^{-1} $\rightarrow$ 6 - 13 Hz 33 - 50 cm^{-1} $\rightarrow$ 13 - 20 Hz

4. BEAM DIVIDER

Many types of beamsplitters have been used in far infrared Fourier spectrometers ranging from the standard dielectric film (usually Mylar), inductive metal mesh and polarisers (free standing wires or metal strips deposited on a thin substrate). However, the dielectric and metal mesh beamsplitters have a limited spectral range and typical efficiencies (4RT) of 60 and 75%, respectively. By comparison, the polariser affords a high efficiency over a broad spectral range. However, as discussed above, in its basic form the polarising FTS detects only one source polarisation and thus 50% of the input spectrum is lost.

Extending previous work in the development of far infrared metal mesh filter technology[10], we have developed an intensity beamsplitter with a high and uniform efficiency over a broad spectral range which is insensitive to source polarisation. The beamsplitter uses two metal meshes in a Fabry-Perot configuration designed to meet the 50% transmission and 50% reflection criteria of an ideal intensity beamsplitter. By using complementary structures (capacitive and inductive grids) on a thin Mylar support substrate we have been able to achieve beamsplitter efficiencies (4RT) above 90% over a range in frequency of a factor of 4. Furthermore, the precise spectral range can be accurately determined by the geometry of the grids and their spacing. One serendipitous feature of these beamsplitters is that the beamsplitters also have 50% transmission and reflection at the HeNe laser wavelength (632.8 nm), which greatly simplifies the alignment of the interferometer. The measured efficiency of the new beamsplitters is shown in Figure 4.

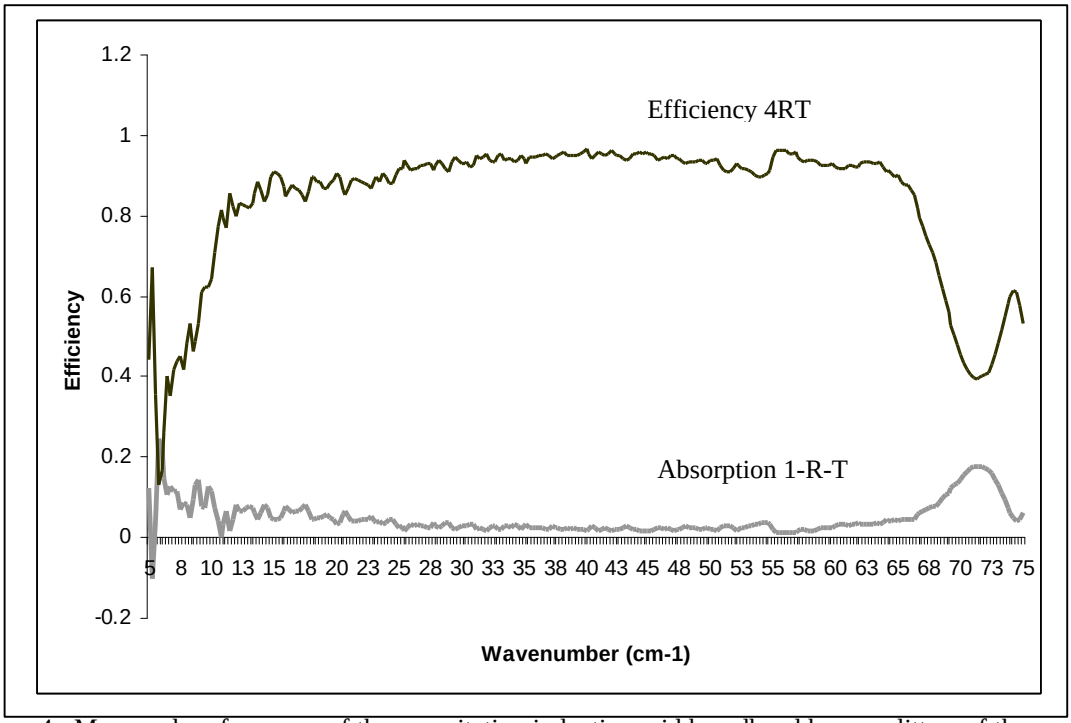

Figure 4: Measured performance of the capacitative-inductive grid broadband beam splitters of the same type that are to be used in the SPIRE FTS

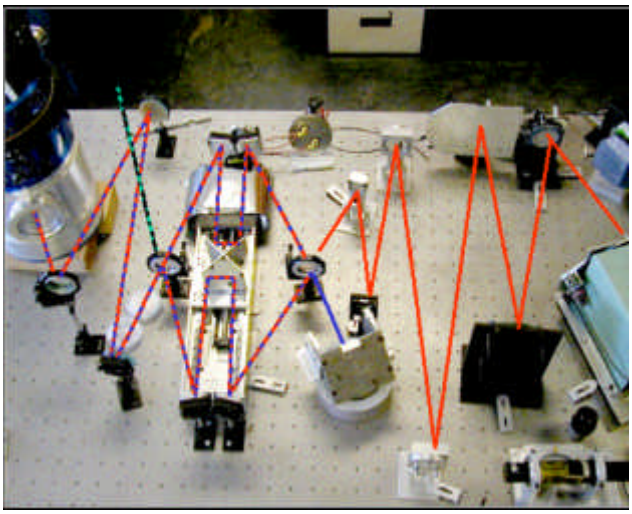

Figure 5: The laboratory demonstrator of the Mach-Zehnder FTS design to be used in the SPIRE instrument. The red line shows the input path from the "sky" port. This enters the interferometer via a telescope simulator and a collimator that produces a beam similar in size to that which pass through the real instrument. The blue line indicates the path from the second input port and the red and blue dashed line the path through the interferometer. Only one exit port has a detector in it in this configuration which is inside the cryostat on the extreme left of the picture.

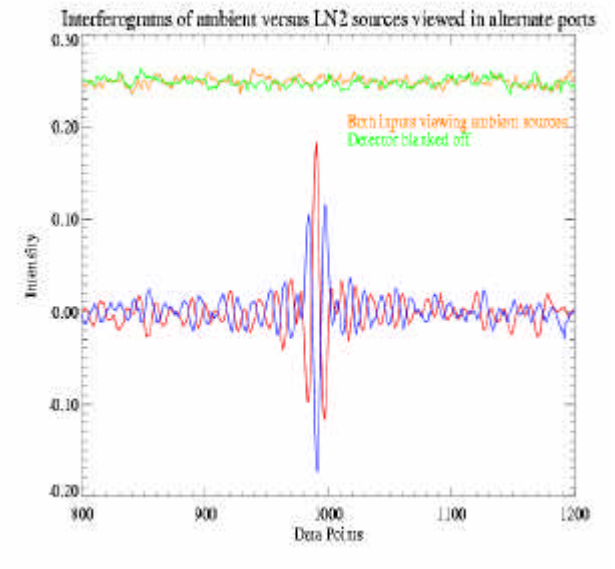

Figure 6: Interferograms of the ambient room background seen against a 77-K target placed in the second input port. The red is for the "sky" port and the blue is for the "calibration" port. The brown line seen above is the co-addition of the two interferograms. The green is the signal seen with the detector blanked off offset for comparison.

5. LABORATORY DEMONSTRATION

In order to demonstrate the operation of the new beam dividers and the principle of the operation of the SPIRE FTS, a laboratory system has been built. This is shown in figure 5. To simply the building of the laboratory demonstrator, the beam is collimated before it enters the interferometer and only plain fold mirrors are used within the collimated section of the beam. The moving mirrors were mounted on a commercial linear stage with a Heidenhain Moiré fringe encoder for the position readout. The detector used was a 1.5-K bolometer. Interferograms have been taken with each of the input ports viewing black room temperature surfaces whilst the other is seeing a 77-K black surface. These are shown in figure 6 together with the resulting signal with the two added together and the signal seen with the detector blanked off. It can be seen that there is little or no residual interferometric signal in the co-added interferograms indicating that each input port is indeed the complement of the other and further that the two arms are very well balanced. As a further test of the spectrometer operation a CO gas cell was placed in the input port before the first beam divider. The CO spectrum is thus seen in absorption against an 800-K black body source. The same cell was also placed in front of a 77-K source in the input port, the relatively warm CO is then seen in emission – see figure 7. A detailed study of the unapodised instrument line shape shows that it fits with the theoretical $(\mathrm{Sinc})^2$ function as expected.

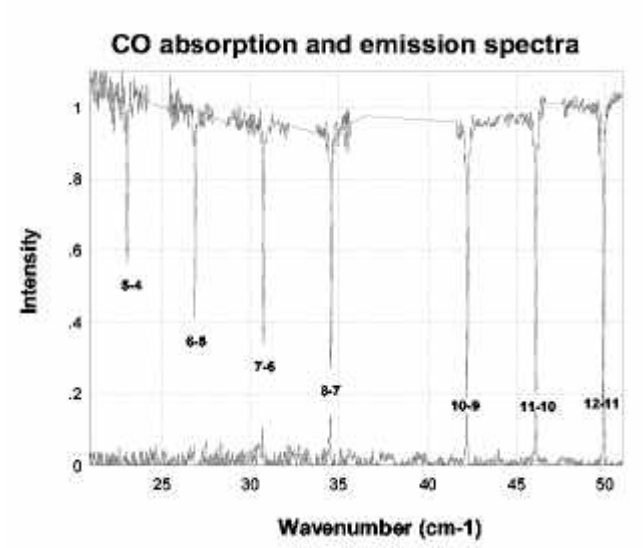

Figure 7: Reconstructed spectra with a CO gas cell placed in the bench top interferometer. The absorption spectrum is with the cell seen against the ambient room background, the emission spectrum (lower trace) is with the cell seen against a 77-K background.

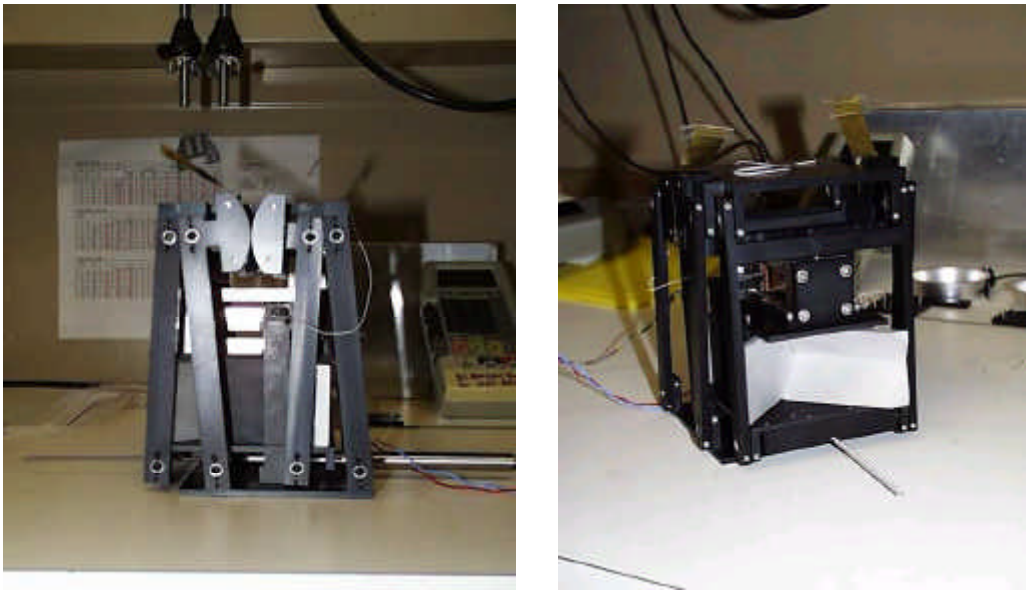

Figure 8: Two views of the prototype mirror carriage built at Goddard Spaceflight Centre showing (left) the double parallelogram mechanism with the "toothless gear" and (right) the mock up of the corner cube mirror. The corner cube compensates the interferometer optics for any tilt or rotation of the mirrors during the mechanism movement.

6. MIRROR MECHANISM

6.1 MIRROR CARRIAGE

The requirements on the mirror mechanism are that it does not shift or tilt the beam during a scan of –0.3 to 3.5 cm and that the position at any point in the scan range can be reconstructed with an accuracy of 0.1 μm. The latter is set by the requirement that the achieved signal to noise in the spectrum is not dominated by position jitter, at least in the case of a compensated signal (see discussion in reference 4 and section 7). A prototype mechanism has been constructed at Goddard Spaceflight Center (GSFC) that is based on a double parallelogram system with a frictionless gear to ensure that the two parallelogram structures move together. Figures 8 shows the side and end views of the prototype mechanism with a commercial actuator fitted and a dummy corner cube mirror.

6.2 POSITION ENCODER

For the position measurement system, a Heidenhain LIP interferential linear encoder[11] is preferred over a linear variable differential transformer (LVDT) transducer for its better accuracy. Cryogenic tests indicate that the Heidenhain encoder may be used at liquid helium temperatures with only minor modifications to the optical head. The optical encoder will have a resolution of 0.1 μm or better and gives a "pulse" as each position is passed rather than an absolute distance measurement. The encoder will be fitted to the outside of the mirror carriage. Measuring the position at a distance from the signal beam imposes stringent requirements on the "nodding" movement of the mirror mechanism, possibly stricter than those imposed by the optical requirements of the spectrometer. The actual value of the requirement will depend on the final configuration of the flight optical encoder and the final carriage design.

6.3 CONTROL SYSTEM AND READOUT

The baseline design of the spectrometer is that it should be operated in "rapid scan" mode with a constant mirror velocity and the time at which each position is passed recorded. The mirror movement will be controlled by a digital feed back loop that uses the time between successive pulses from the optical encoder to control the speed of the mirrors. In order that the mirror velocity jitter in the signal detection band (essentially 0.03-25 Hz) does not affect the achieved signal to noise, the feedback loop will be operated at about 2 kHz. The digital feedback loop will be implemented using a digital signal

processor, most likely the TEMIC TSC21020 type that is already baselined for the instrument on board computer. The detectors could be read out in one of two methods given the encoder type we plan to implement:

Position sampling with synchronised detector readout. In this scenario the mirror position pulse is used to trigger the readout of the detectors. The time taken to readout the detector array will need to include any possible uncertainty in the time interval between positions due to the uncertainty in the mirror velocity. This method has the advantage that each frame will be recorded at a known mirror position within the uncertainty of the mirror velocity from one position sample to the next. This means the interferograms can be safely co-added with no need to interpolate the data onto a common position grid. The disadvantage of this method is that it requires both a synchronisation pulse from the mirror drive electronics to the detector read-out electronics (and therefore makes the electronics more complicated) and a higher readout rate for the detectors.

Time sampling. Here the time of each pulse from the position sensor is recorded and the detectors are independently sampled; with perhaps a start pulse at the start of the scan to synchronise the readout. The advantage of this scenario is that it is simpler to implement in the electronics and will be less prone to operational difficulties associated with timing between the position readout and detector readout. The disadvantage is that, because of the uncertainty in the mirror velocity and any hysteresis or scan to scan variability in the positioning of the mirror, the detector readouts will have to be interpolated onto a common position grid before co-addition of the interferograms. In practical terms this will probably prevent on board co-addition of the interferograms and the mirror scan speed will therefore have to be adjusted to allow the data sampling rate to fit within the 100 kbit/second telemetry bandwidth available for the FIRST instruments.

After an assessment of the implementation of the two methods in the electronics system for the SPIRE instrument, it was decided to adopt the time sampling method as the default operating mode. The impact of this on the performance of the instrument has been simulated and is reported in section 7.

7. PERFORMANCE SIMULATIONS

7.1 INSTRUMENT SENSITIVITY

A radiometric model of the SPIRE instrument has been constructed and the results are reported by Griffin et al[2]. This shows that, given the estimated throughput of the FTS filters and optics and a detector noise equivalent power (NEP) of $3x10^{-17}$ W $Hz^{-1/2}$, the instrument NEP for the FTS will be between $1.4x10^{-16}$ and $1.8x10^{-16}$ W $Hz^{-1/2}$. This is equivalent to a 1-σ in 1 hour detection sensitivity of about $6x10^{-18}$ W m^{-2} in the 200-400 μm band for the under-illuminated telescope diameter of 3.28 m. However, this level of sensitivity will only be reached if the noise in the interferograms is truly dominated by the photon noise from the telescope background. To evaluate what performance is required from the velocity control system of the mirrors to ensure that the instrument remains background noise limited and not limited by noise induced by the mirror scan mechanism control, we have performed a number of computer simulations of the instrument performance.

7.2 POSITION ERROR AND COMPENSATION

The initial simulations showed that the mirror position measurement accuracy had to be better than a few tens of nanometres if the signal to noise on the uncompensated signal was to be photon noise limited. This level of accuracy will be very difficult to achieve within the envelope and resources available for the SPIRE instrument. If the signal is compensated to reduce the dynamic range of the ZPD peak then a position accuracy of a few hundred nanometres, such as could be provided by either a Heidenhain optical encoder or an LVDT, could be sufficient to ensure that the mechanism does not dominate the noise. Simulations have been run to check what level of compensation is required to reduce the dynamic range of the detectors sufficiently to ensure that position accuracy of the order of a few hundred nanometres position accuracy is sufficient at the highest observed frequency. A reduction in the dynamic range of the ZPD signal of a factor of 20 was calculated to be sufficient to prevent the position error dominating the signal to noise in the interferogram. For safety we have set a requirement of 400 nanometres position accuracy in OPD for a signal compensated to at least 5% of the signal from the telescope alone. This is equivalent to 100 nanometres for the actual mirror position measurement (see section 6). We have calculated that a 75 K 4% emissivity calibration source will provide give at least 95% compensation at all wavelengths for the spectrum of the 80 K 4% emissivity telescope.

7.3 VELOCITY CONTROL SIMULATION

The effect of the combination of velocity control error and the frequency response of the detector and electrical filtering may still cause problems with the achieved signal to noise in an interferogram. To test for these effects, a further simulation has

been carried out using a program written in IDL[12] to simulate the behaviour of a Mach-Zehnder FTS. The program takes in both the "sky port" spectrum – this can include a simulated astronomical source and the telescope background – and the "calibration port" spectrum. The simulation accounts for all the operating parameters of the FTS including the uncertainty in the position measurement; sampling; velocity; detector frequency response; detector and photon noise and electrical filtering. In the simulation the position of the mirrors at each sampling point has a random error associated with it to replicate the measurement inaccuracy in the encoder. The optical path difference output by the program is "perfect" whilst that used for the calculation of the signal has a random error added to it. The time at which each position is reached is initially calculated from the position with its associated error assuming a fixed mirror velocity. The velocity control is further simulated as a sinusoidal variation with time at a fixed frequency and amplitude. The signal seen from the sky port and the calibration port is calculated separately for each of the two output ports.

To run simulations of the effect of velocity error on the final signal-to-noise an interferogram was generated with a high degree of oversampling and the OPD measurement uncertainty set at 400 nanometres. The sinusoidal velocity error was then imposed on the timing of the samples and the signal rolled off according to the time constant of the detector. This signal was resampled at a fixed time interval to simulate the time sampling to be used for SPIRE. A fixed array of mirror positions was also generated with the interval set to the position sampling interval required for the degree of oversampling to be used in SPIRE. The time each fixed mirror position was passed was recorded.

To complete the simulation some noise was added to the signal in the form of fixed detector noise and photon noise. The fixed detector noise was taken as 3.2 nV $Hz^{-1/2}$ and the photon noise estimated as that on the mean signal in the interferogram referred to the input of the pre-amplifier – i.e. converted to volts. Both were assumed to be white and after addition of the noise both the signal and the noise were rolled off by a simulated electrical filter in frequency space before conversion back the time domain. The filter was set as having a cut off at 28 Hz and a -60 dB per decade slope thereafter.

The final stage in the program is to convert the interferogram into a spectrum. The error in the velocity means that more signal samples are taken than needed and there is no one to one correspondence between the position and the signal sample. The "true" optical path difference at each sample is therefore reconstructed by a linear interpolation of the measured optical difference versus time onto the fixed time grid of the signal sampling (other methods may be more optimal, for the present purposes this is sufficient). To look at the effect of velocity instability on the signal to noise the whole procedure is repeated ten times for a given set of input parameters. The signal to noise in the final spectrum is then computed by averaging all ten spectra and taking the standard deviation at each wavenumber sample.

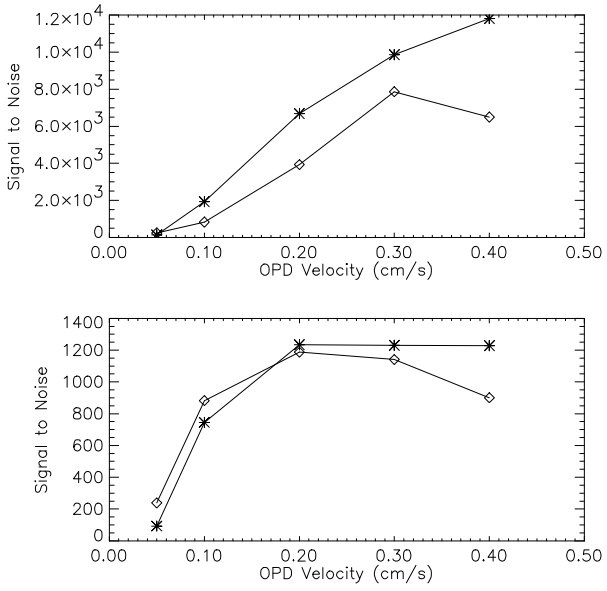

Figure 9: Signal to noise versus mirror speed with the velocity error amplitude set at 0.02 cm/s. The stars are for the 30 to 40 cm^{-1} optical band and the diamonds for the 40 to 50 cm^{-1} optical band. The upper panel is the uncompensated signal and the lower the compensated signal.

7.4 EFFECT OF VELOCITY ERROR

To test the effect of the mirror speed on the signal to noise in the spectrum, the program was run with the velocity sinusoid frequency set at 175 Hz; the velocity error amplitude fixed at 0.02 cm/s and the mean velocity varied between 0.05 and 0.4 cm/s. A fixed amplitude was used here rather than a fixed percentage of the mirror velocity as this more nearly simulates the predicted performance of the FTS control system which will achieve a given fixed velocity error rather than the same percentage error for all velocities. The results for signal to noise are shown in figure 9. Here the mean signal to noise ratio has been calculated over two sub-bands of a simulated short wavelength filter (see figures 10 and 11) – 30-40 cm^{-1} and 40-50 cm^{-1}. The telescope is represented as an 80 K 4 % emissive black body and the calibration source as a 75 K 4% emissive black body.

One can see that the uncompensated signal to noise reduces almost linearly with decreasing velocity as the fractional error increases. The compensated signal does not suffer as badly even for velocities down to 0.1 cm/s (implying a 20% error in the velocity). The signal to noise is seen to be reduced in the higher frequency sub-band for the

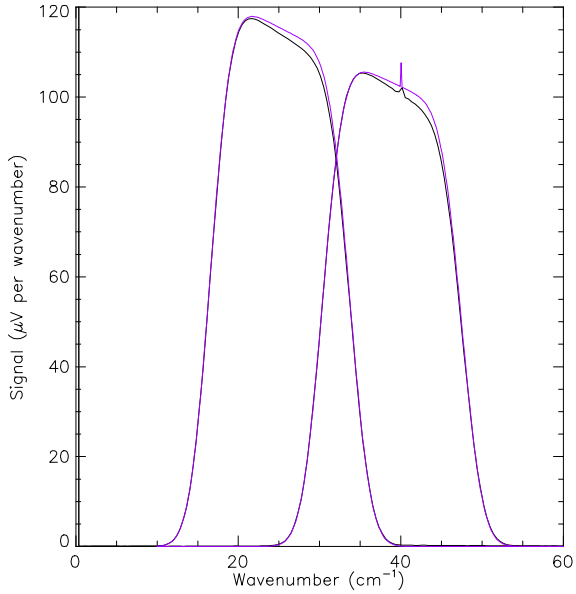

Figure 10: The reconstructed uncompensated spectrum versus wavenumber in both channels with the FTS working with the default operating parameters: OPD velocity 0.2 cm/s; velocity error 0.02 cm/s and velocity error frequency >100 Hz.

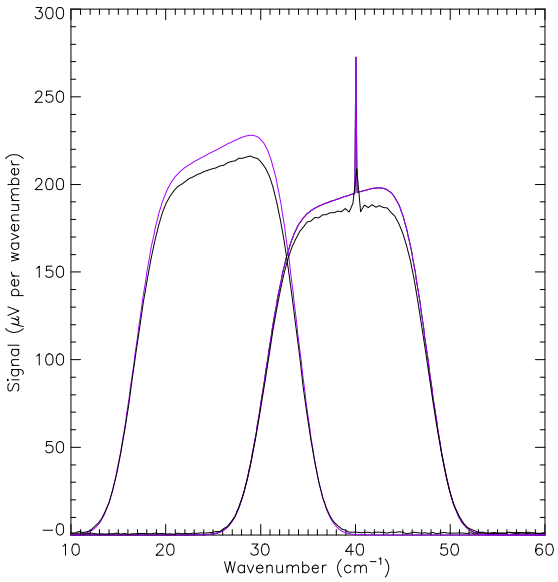

Figure 11: The reconstructed compensated spectrum versus wavenumber in both channels with the FTS working with the default operating parameters. The simulated filters used are somewhat narrower than will be used in practice, as we would wish to have good response out to 50 cm^{-1}.

uncompensated case. The signal to noise in this band also decreases for the highest velocity in both the compensated and uncompensated cases. This reflects the roll off in responsivity of the detectors as the audio band approaches the detector frequency response. Both this effect and the effects of velocity and position error are amplified by the large signal differential close to the ZPD when the signal is not compensated. Some distortion of the spectrum will also be caused by not phase correcting the interferogram for the effects of the detector frequency response. These effects are ameliorated when the signal is compensated as the signal differential close to the ZPD is much reduced.

Figures 10 and 11 show the reconstructed and input spectra for both the channels for the uncompensated and compensated signals for the velocity set at 0.2 cm/s and the resolution set at 0.4 cm^{-1}. In both cases the spectral shape is well reproduced and the difference between input and reconstructed spectra is due in part to uncorrected phase errors caused by the detector frequency response. For this simulation the telescope was represented as an 80 K 4% emissive blackbody; the calibrator as a 75 K 4% emissive black body and the "source" as a 40 K 100% emissive black body with an angular extent of 3 arcseconds. A line very much narrower than the resolution element of the spectrometer was placed at 40 cm^{-1}. Comparison of figures 10 and 11 shows that, whilst the total power on the detectors has increased, the contrast on the source spectrum is much enhanced in the compensated case.

7.5 SELECTION OF OPERATING PARAMETERS

In order to maintain the background limited performance of the FTS it is clear that the compensation of the signal from the telescope is extremely important to reduce the effects of position inaccuracy and velocity jitter. Never-the-less we cannot completely rely on the compensation source as it may fail during launch or in flight. We must therefore set the operating parameters so that we can still operate efficiently if we lose the calibrator. The results of the simulations reported here show that the following parameters for the operation of the SPIRE FTS will ensure that, although compensation of the signal is highly desirable, the FTS will still perform adequately if the calibration source fails:

Oversampling of the mirror position:	4
Average mirror velocity:	0.05 cm/s (equivalent to 0.2 cm/s OPD)
Velocity jitter frequency:	>100 Hz (4 times higher than the highest detectable frequency)

Detection band:	30 mHz to 28 Hz for detector 3 dB response of 20 Hz
Equivalent audio frequencies:	2.5 to 10 Hz (15 to 50 cm^{-1})
Velocity jitter amplitude:	<0.005 cm/s (equivalent to 0.02 cm/s OPD)

8. CONCLUSIONS

We have described a novel far infrared and sub-millimetre imaging Fourier Transform Spectrometer based on the Mach-Zehnder principle with broadband intensity beam splitters. This spectrometer is due to be flown on the FIRST mission as part of the SPIRE instrument. The optical design has been tailored to the space available within the focal plane enclosure of FIRST and, whilst it is compact, still allows for an instrument field of view of 2.6 arcmin and a maximum resolution of 0.04 cm^{-1}. A laboratory demonstration of the principle of operation of the new interferometer has been built and tested. This shows that the design is robust against alignment inaccuracies and that twin broadband intensity dividing beam splitters can be used in the FIR and sub-millimetre with excellent results. The feedhorn bolometer arrays to be used in the instrument will give a large instantaneous signal from the relatively warm FIRST telescope and a compensating calibration source is required to achieve background limited sensitivity. However, the fast speed of response of the these detectors combined with their excellent low frequency stability means that the mirror velocity can be adjusted to minimise the impact of predicted velocity control errors and position measurement uncertainty.

9. REFERENCES

1. G. Pilbratt, “The FIRST mission: baseline, science objectives and operations”, *Proceedings of ESA Symposium on The Far Infrared and Submillimetre Universe*, Grenoble, 15-17 April 1977, ESA SP-401, pp 7-12, 1997.
2. M. Griffin, L. Vigroux, B. Swinyard, “The SPIRE instrument for FIRST”, Proc. SPIE **4013** (this volume), Munich, 27-31 March (2000).
3. J. J. Bock, H. G. LeDuc, A. E. Lange, and J. Zmuidzinas, “A monolithic bolometer array suitable for FIRST”, *Proceedings of ESA Symposium on The Far Infrared and Submillimetre Universe*, Grenoble, 15-17 April 1977, ESA SP-401, pp 349-352, 1997.
4. K. Dohlen, A. Origné, D. Pouliquen, B. Swinyard, “Optical design of the SPIRE instrument for FIRST”, Proc. SPIE **4013** (this volume), Munich, 27-31 March 2000.
5. M. E. Caldwell, B. M. Swinyard, A. Richards, “Beam pattern (diffraction) aspects in design of the SPIRE instrument”, Proc. SPIE **4013** (this volume), Munich, 27-31 March 2000.
6. A. Poglitsch, N. Geis, C. Waelkens, “Photoconductor array camera and spectrometer (PACS) for FIRST”, Proc. SPIE **4013** (this volume), Munich, 27-31 March 2000.
7. S. Beckwith et al, “FIRST – Far InfraRed and Submillimetre Space Telescope”, *ESA SCI(93)6*, 1993
8. “The High Frequency Instrument for the Planck mission - proposal submitted in response to the ESA announcement of opportunity”, http://sci.esa.int/planck
9. P.A.R. Ade, P. Hamilton, D.A. Naylor, "An Absolute Dual Beam Emission Spectrometer", *Fourier Transform Spectroscopy: New Methods and Applications*, OSA, **90**, 1999.
10. C. Lee, P.A.R. Ade, C.V. Haynes, “Self Supporting Filters for Compact Focal Plane Designs”, *Proceedings of the 30th ESLAB Symposium*, ESTEC, Noordwijk, The Netherlands, Sept. 1996,
11. *Exposed linear encoders*, http://www.heidenhain.com/Products/ExposedLinear/lip.htm
12. *Interactive Data Language*, Research Systems Inc., http://www.rsinc.com